

Para-ortho transition of artificial H₂ molecule in lateral quantum dots doped with magnetic impurities

Ramin M. Abolfath

Department of Radiation Oncology, University of Texas Southwestern Medical Center, Dallas, Texas 75390, USA

(Dated: April 25, 2022)

We present the magnetic phase diagram of artificial H₂ molecule in lateral quantum dots doped with magnetic impurities as a function of external magnetic field and plunger gate voltage. The onset of Mn-Mn antiferromagnetic-ferromagnetic transition follows the electron spin singlet-triplet transition. We deploy a configuration-interaction method to exactly diagonalize the electron-Mn Hamiltonian and map it to an effective Mn-Mn Heisenberg Hamiltonian. We find that Mn-Mn exchange coupling can be described by RKKY-interaction/magnetic-polaron in weak/strong electron-Mn coupling at low/high magnetic fields.

PACS numbers: 75.75.+a,75.50.Pp,85.75.-d

I. INTRODUCTION

There is currently significant experimental^{1,2,3,4,5,6,7} and theoretical^{8,9,10,11,12,13,14} interest in semiconductor quantum dots (QDs) doped with magnetic impurities. Fabrication of hybrid systems consisting magnetic ions in a controlled electronic environment provides an interesting interplay between interaction effects and magnetism. In particular the application of spin of electrons in quantum dot molecules for generation of electron entanglement and quantum information processing in solid state devices is of current interest^{15,16}. One of the challenges in use of spin of electrons in scalable quantum computer devices is the spin dephasing due to interference by spin-orbit coupling and nuclear hyperfine interaction¹⁷. The broadening of the electron envelop wavefunction in a QD is determined by the length scale of the confining potential that is comparable with the size of QD (typically ≈ 1 -1000 nm). In materials with high abundance of spin-carrying nuclear isotopes, the electron interacts with large number of nuclei in host semiconductor. Although the strength of nuclear hyperfine coupling is small (typically $\approx 1\mu\text{eV}$) compare to other relevant energy scales, but because of the broadening of the confined electron in nano-meter length scale, it interacts with a large number of nuclei that contribute to the electron spin dephasing. The use of magnetic moment of nuclear impurities in host semiconductors for the quantum information processing have appeared to overcome this limitation^{18,19}. Recently the system of ¹³C atoms in two-electron nanotube quantum dot molecules has been studied²⁰. The advantage of using singlet eigen-states of coupled magnetic moments of nucleus of ¹³C in organic molecules and their effects in dramatic enhancement of the spin life-times needed for imaging the metabolic pathways in living systems by hyperpolarization methods has been investigated²¹. Moreover, molecules doped with ¹³C has been used in demonstration of quantum teleportation using NMR techniques¹⁸. Similarly the magnetic dipole moment of nucleus of ³¹P-impurities in Si-based quantum computer model proposed by Kane¹⁹ appears to be

promising in making quantum computer solid state devices. Similar to magnetic dipole moment of nucleus of ¹³C and/or ³¹P, the magnetic moment of electrons in *d*-shell of magnetic impurities (such as Mn, Fe, Co) in lateral quantum dot molecules can be used for quantum information processing as they have been used for fabrication of molecular magnets²².

In this work we focus on theoretical study of the phase diagram and spin transitions of coupled magnetic impurities (e.g. Mn) doped in two electron quantum dot molecule, an artificial H₂ molecule. Here we calculate the Mn-Mn effective Hamiltonian mediated by electrons and show that the onset of spin-polarized state with finite Mn-magnetization, corresponds to spin singlet-triplet transition of two electrons in QD molecule. This transition is analogous to para-ortho transition of nucleus of solid H₂ where the electron-nuclei hyperfine interaction opens the energy gap between para and ortho states of H₂ molecule^{24,25}. In the small (large) magnetic fields the spin singlet (triplet) state is the ground state of electrons¹⁶ and thus the ground state of the coupled Mn is described by hydrogen molecule para (ortho) state. In the small magnetic fields the Mn-Mn interaction induced by electrons is calculated perturbatively in the electron-Mn weak interacting limit. It can be described effectively by RKKY-coupling²³. In large magnetic field the ground state of electrons is spin-triplet. The electron-Mn interaction is strong and magnetic-polaron state form. In this limit the ortho-state of artificial H₂ molecule is stable. We show the Mn-Mn exchange coupling can be controlled by inter and intra dot correlations, external magnetic field and gate voltage. The dependence of Mn-Mn interaction to the external gate voltage and magnetic field mediated by spin singlet-triplet transition among electrons in QDs opens up the possibility in using Mn-magnetic moment as qubit in quantum computation purposes. In contrast to electrons confined in QDs, because of highly localized *d*-electrons, Mn's interact directly with significantly smaller number of nuclei in host semiconductor. The Mn *d*-electrons also do not interact directly with the host semiconductor Rashba and Dresselhaus spin-orbit coupling²⁸, and thus their spin coherence life-time

is expected to be longer than the QD electrons. However, Mn-Mn interaction mediated by electrons in QDs are still vulnerable to the electron spin dephasing mediated by QD electrons due to their hyperfine and spin-orbit couplings. In analogous to the ^{31}P in Si system¹⁹, the spin coherence time in the Mn system is expected to be longer than the QD electron system. Further investigation is required to make a quantitative dependence of spin decoherence time of Mn on the electron-nuclear hyperfine interaction and their spin-orbit coupling.

II. HAMILTONIAN

We represent magnetic QD molecule by the Hamiltonian $H = H_e + H_{em} + H_m$, describing contributions of interacting electrons, electron-Mn (e-Mn) exchange, and direct Mn-Mn antiferromagnetic (AFM) coupling, respectively. Electrons confined in quasi-two-dimensional quantum dots in a uniform perpendicular magnetic field can be described by the effective mass Hamiltonian

$$H_e = \sum_{i=1}^N (T_i + E_{iZ}) + \frac{e^2}{2\epsilon} \sum_{i \neq j} \frac{1}{|\vec{r}_i - \vec{r}_j|}, \quad (1)$$

where

$$T = \frac{1}{2m^*} \left(\frac{\hbar}{i} \vec{\nabla} + \frac{e}{c} A(\vec{r}) \right)^2 + V(x, y) \quad (2)$$

is the single electron Hamiltonian in magnetic field. Here $(\vec{r}) = (x, y)$ describes electron position, $V(\vec{r})$ is the quantum dots confining potential, $A(\vec{r}) = \frac{1}{2} \vec{B} \times \vec{r}$ is the vector potential, and B is the external magnetic field perpendicular to the plane of confining potential. m^* is the conduction-electron effective mass, $-e$ is the electron charge, and ϵ is the host semiconductor dielectric constant. $E_{iZ} = \frac{1}{2} g_e \mu_B \sigma_{iz} B$ is the Zeeman spin splitting, g_e is the electron g-factor in host semiconductor, μ_B is the Bohr magneton, and σ is the Pauli matrix. The single particle eigenvalues ($\epsilon_{\alpha\sigma}$) and eigenvectors ($\varphi_{\alpha\sigma}$) are calculated by discretizing T in real space, and diagonalizing the resulting matrix using conjugated gradient algorithm^{16,26}. The single-particle (SP) states can be used as a basis in configuration-interaction (CI) calculation that allows to diagonalize Hamiltonian H . The details of CI method can be found in Ref.²⁶. Denoting the creation (annihilation) operators for electron in non-interacting SP state $|\alpha\sigma\rangle$ by $c_{\alpha\sigma}^\dagger$ ($c_{\alpha\sigma}$), the Hamiltonian of an interacting system in second quantization can be written as

$$H_e = \sum_{\alpha} \sum_{\sigma} \epsilon_{\alpha\sigma} c_{\alpha\sigma}^\dagger c_{\alpha\sigma} + \frac{1}{2} \sum_{\alpha\beta\gamma\mu} \sum_{\sigma\sigma'} V_{\alpha\sigma,\beta\sigma',\gamma\sigma',\mu\sigma} c_{\alpha\sigma}^\dagger c_{\beta\sigma'}^\dagger c_{\gamma\sigma'} c_{\mu\sigma}, \quad (3)$$

where the first term represents the single particle Hamiltonian Eq.(2), and $V_{\alpha\sigma,\beta\sigma',\mu\sigma',\nu\sigma} =$

$\int d\vec{r} \int d\vec{r}' \varphi_{\alpha\sigma}^*(\vec{r}) \varphi_{\beta\sigma'}^*(\vec{r}') \frac{e^2}{\epsilon|\vec{r}-\vec{r}'|} \varphi_{\mu\sigma'}(\vec{r}') \varphi_{\nu\sigma}(\vec{r})$, is the two-body Coulomb matrix element. We describe e-Mn exchange interaction by $H_{em} = -J_{sd} \sum_{i,I} \vec{s}_i \cdot \vec{M}_I \delta(\mathbf{r}_i - \mathbf{R}_I)$, where J_{sd} is the exchange coupling between electron spin \vec{s}_i at \mathbf{r}_i and impurity spin \vec{M}_I at \mathbf{R}_I ^{10,11}. Note that H_{em} is analogous of the isotropic (contact) part of electron-nucleus hyperfine interaction²⁷, responsible for para-ortho energy gap of solid H_2 (for comparison see for example eq. 121.9, page 498 of Ref.²⁴). In second quantization it can be written as

$$H_{em} = - \sum_{\alpha\beta} \sum_I \frac{J_{\alpha\beta}(\mathbf{R}_I)}{2} [M_{zI} (c_{\alpha\uparrow}^\dagger c_{\beta\uparrow} - c_{\alpha\downarrow}^\dagger c_{\beta\downarrow}) + M_I^+ c_{\alpha\downarrow}^\dagger c_{\beta\uparrow} + M_I^- c_{\alpha\uparrow}^\dagger c_{\beta\downarrow}], \quad (4)$$

where $J_{\alpha\beta}(\mathbf{R}_I) = J_{sd} \varphi_{\alpha}^*(\mathbf{R}_I) \varphi_{\beta}(\mathbf{R}_I)$. Finally we describe Mn-Mn direct exchange interaction and Mn-Zeeman coupling by $H_m = \sum_{I,I'} J_{I,I'}^{AF} \vec{M}_I \cdot \vec{M}_{I'} + \sum_I g_m \mu_B M_{Iz} B$, where $J_{I,I'}^{AF}$ is the direct Mn-Mn AFM coupling¹⁰, resembling the direct dipole-dipole interaction, and g_m is the Mn g-factor.

A. Confining potential

For numerical calculation we model quantum dots molecules by the following confining potential $V(x, y) = V_L \exp[-\frac{(x+a)^2+y^2}{\Delta^2}] + V_R \exp[-\frac{(x-a)^2+y^2}{\Delta^2}] + V_p \exp[-\frac{x^2}{\Delta_{Px}^2} - \frac{y^2}{\Delta_{Py}^2}]$. Here V_L, V_R describe the depth of the left and right quantum dot minima located at $x = -a, y = 0$ and $x = +a, y = 0$, and V_p is the plunger gate potential controlled by the central gate²⁶. For identical dots, $V_L = V_R = V_0$, and confining potential exhibits inversion symmetry. Our numerical results are calculated for parameters based on (Cd,Mn)Te QDs with $J_{sd} = 0.015$ eV nm³, $m^* = 0.106$, $\epsilon = 10.6$, $g_m = 2.02$, $g_e = -1.67$ and the effective Bohr radius $a_B^* = 5.29$ nm and Rydberg energy $Ry^* = 12.8$ meV. We parametrize the confining potential by $V_0 = -10$, $a = 2$, $\Delta = 2.5$, and $\Delta_{Px} = 0.3$, $\Delta_{Py} = 2.5$, in effective atomic units. V_p , which controls the potential barrier, varies to control the inter-dot correlations, independent of the locations of the quantum dots. The choice of parameters ensures weakly coupled quantum dots.

III. TWO LEVEL SYSTEM

For the purpose of this work we consider a coupled quantum dot system filled with two electrons. It is convenient to project the Hilbert space of two electrons into a two level system. The construction of two level system based on single particle orbitals localized in each dot is made by defining a pair of bonding-anti-bonding single particle orbitals $\varphi_{\pm}(\vec{r}) = [\varphi_L(\vec{r}) \pm \varphi_R(\vec{r})] / \sqrt{2(1 \pm W)}$,

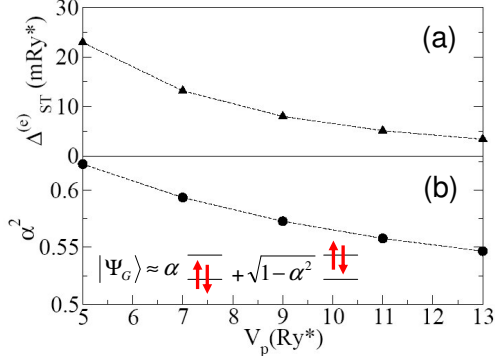


FIG. 1: (Color online) (a) Shown singlet-triplet energy gap ($\Delta_{ST}^{(e)}$) of two electrons in a coupled quantum dot molecule as a function of plunger gate voltage (V_p) at $B = 0$. (b) Shown α^2 as a function of V_p .

where $\varphi_{L(R)}(\vec{r})$ is the spatial part of SP wave-function localized in L (R) dot, and $W = Re(\langle L|R \rangle)$ is the overlap integral. At zero (finite) magnetic field the SP orbitals are real (complex) functions. At $H_{em} = B = 0$ the lowest energy many body wave function (ground state) of two electrons is spatially symmetric with parity +1. Thus spin state of the ground state must be singlet: $\Psi_G(\vec{r}_1, \vec{r}_2) = [\alpha\varphi_+(\vec{r}_1)\varphi_+(\vec{r}_2) + \beta\varphi_-(\vec{r}_1)\varphi_-(\vec{r}_2)]|S_0\rangle$, where $\beta = \sqrt{1-\alpha^2}$ and $|S_0\rangle = (|\uparrow\downarrow\rangle - |\downarrow\uparrow\rangle)/\sqrt{2}$ corresponding to $S = S_z = 0$. Here S is the total spin of two electrons. The lowest energy excited states are the spin-triplet states with spatially antisymmetric wave-function corresponding to parity -1, and $\Psi_X^\sigma(\vec{r}_1, \vec{r}_2) = \frac{1}{\sqrt{2}}[\varphi_+(\vec{r}_1)\varphi_-(\vec{r}_2) - \varphi_+(\vec{r}_2)\varphi_-(\vec{r}_1)]|T_\sigma\rangle$. Here $\sigma = 0, \pm 1$, and $|T_\sigma\rangle$ is one of the spin-triplet states: $|T_{+1}\rangle = |\uparrow\uparrow\rangle$, $|T_0\rangle = (|\uparrow\downarrow\rangle + |\downarrow\uparrow\rangle)/\sqrt{2}$, and $|T_{-1}\rangle = |\downarrow\downarrow\rangle$ corresponding to $S = 1$, and $S_z = +1, 0, -1$ respectively. Note that at $B = 0$ (or zero Zeeman coupling) these states are degenerate and thus Ψ_X^σ is three-fold degenerate. We define spin singlet-triplet energy gap of electrons $\Delta_{ST}^{(e)} \equiv E_X^{(e)} - E_G^{(e)}$ where $H_e|\Psi_G\rangle = E_G^{(e)}|\Psi_G\rangle$, and $H_e|\Psi_X^\sigma\rangle = E_X^{(e)}|\Psi_X^\sigma\rangle$. In this two level system there are two other excited states with spin-singlet $\Psi_X^{s1}(\vec{r}_1, \vec{r}_2) = [\beta\varphi_+(\vec{r}_1)\varphi_+(\vec{r}_2) - \alpha\varphi_-(\vec{r}_1)\varphi_-(\vec{r}_2)]|S_0\rangle$, and $\Psi_X^{s2}(\vec{r}_1, \vec{r}_2) = \frac{1}{\sqrt{2}}[\varphi_+(\vec{r}_1)\varphi_-(\vec{r}_2) + \varphi_+(\vec{r}_2)\varphi_-(\vec{r}_1)]|S_0\rangle$.

A. Weak e-Mn coupling

Assuming the weak electron-Mn interaction limit, we calculate Mn-Mn effective Hamiltonian mediated by elec-

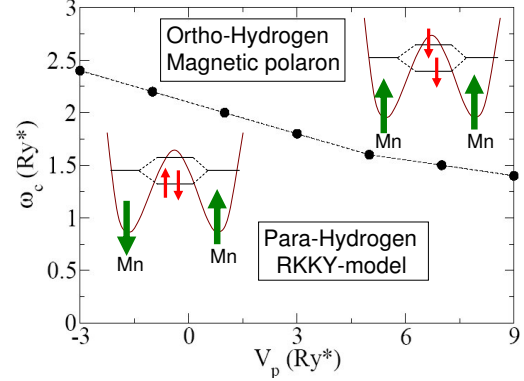


FIG. 2: (Color online) Spin singlet-triplet phase diagram calculated by configuration interaction method for two electrons in lateral quantum dot molecules.

trons perturbatively. In this limit H_{em} is assumed to be small, compared to unperturbed Hamiltonian H_e . In the low magnetic field limit, the ground state of two electrons in coupled quantum dot is spin-singlet. It follows

$$H_{mmm}^{\text{eff}} = \sum_X \frac{|\langle \Psi_X | H_{em} | \Psi_G \rangle|^2}{E_G^{(e)} - E_X^{(e)}}. \quad (5)$$

Here G and X denote the ground and excited states of electrons in quantum dot systems, and $X \in \{\Psi_X^{s1}, \Psi_X^{s2}, \Psi_X^{0,\pm 1}\}$. The uniqueness (non-degeneracy) of the ground state has been assumed implicitly. To obtain effective interaction between two Mn, we calculate the matrix elements of H_{em} . It is straightforward to show that $\langle \Psi_X^{s1} | H_{em} | \Psi_G \rangle = \langle \Psi_X^{s2} | H_{em} | \Psi_G \rangle = 0$, $\langle \Psi_X^0 | H_{em} | \Psi_G \rangle = \frac{\lambda J_{sd}}{\sqrt{2}} \sum_I \Phi(\vec{R}_I) M_I^z$, $\langle \Psi_X^{+1} | H_{em} | \Psi_G \rangle = -\frac{\lambda J_{sd}}{2} \sum_I \Phi(\vec{R}_I) M_I^-$, and $\langle \Psi_X^{-1} | H_{em} | \Psi_G \rangle = +\frac{\lambda J_{sd}}{2} \sum_I \Phi(\vec{R}_I) M_I^+$, where $\lambda = \alpha - \beta$ and $\Phi(\vec{R}_I) \equiv \varphi_+(\vec{R}_I)\varphi_-(\vec{R}_I)$. We finally find

$$H_{mmm}^{\text{eff}} = \sum_{I,I'} \Delta_{II'} \vec{M}_I \cdot \vec{M}_{I'}, \quad (6)$$

where $\Delta_{II'} = -\frac{\lambda^2 J_{sd}^2}{2\Delta_{ST}^{(e)}} \varphi_L^2(\vec{R}_I)\varphi_R^2(\vec{R}_I)\varphi_+(\vec{R}_I)\varphi_-(\vec{R}_I)$. Note that the Mn-Mn coupling for a lateral quantum dot molecule with two magnetic impurities localized at the center of each dot is given by

$$\Delta_{12} = +\frac{\lambda^2 J_{sd}^2}{2\Delta_{ST}^{(e)}} \frac{\varphi_L^2(\vec{R}_1)\varphi_R^2(\vec{R}_2)}{4(1-W^2)} > 0. \quad (7)$$

Here we assume that \vec{R}_1 and \vec{R}_2 are the position of Mn's centered at left and right dots, and therefore the elec-

tron wave-functions at the opposite position of Mn's, $\varphi_L^2(\vec{R}_2)$ and $\varphi_R^2(\vec{R}_1)$ are negligible due to high localization of the wave-functions. Because Δ_{12} is positive, the coupling between two Mn mediated by electrons is anti-ferromagnetic with $M = 0$ as the ground state. For Mn, this state is separated by an energy gap, $30\Delta_{12}$, from the ferromagnetic state $M = M_1 + M_2 (= 5)$. There are series of canted states with $M = 1, \dots, 4$ between $M = 0$ and $M = 5$.

IV. EXACT DIAGONALIZATION

The effect of V_p at $B = 0$ on both α and $\Delta_{ST}^{(e)}$ is shown in Fig. 1. This calculation is based on CI method using 20 SP-orbitals (400 electronic configurations). With increasing V_p the inter dot tunneling and the overlap between L and R wave-functions decreases. This results to the decrease of α (hence λ) and $\Delta_{ST}^{(e)}$ simultaneously. The expansion of the ground state wave function $|\Psi_G\rangle$, in terms of leading configurations of two electrons is shown. The contribution of the rest of configurations is negligible.

With increase of magnetic field, the electron spin singlet-triplet energy gap $\Delta_{ST}^{(e)}$ decreases. Close to the transition point, $\Delta_{ST}^{(e)}$ vanishes, and the perturbation method fails. An unperturbative approach has to develop to calculate the low lying energy states of H in order to map H into H_{mm}^{eff} . Here we exactly diagonalize Hamiltonian H by expanding the many body wave-function in the basis of electron-Mn configurations: $|\Psi, M\rangle = c_{\alpha\sigma}^\dagger c_{\beta\sigma'}^\dagger |0\rangle \otimes |M_{z1}, M_{z2}\rangle$. Because of $[S_z, H_{em}] \neq 0$, (S is the total spin operator of two electrons), the states with different S_z are mixed, hence the dimension of matrix H that has to be diagonalized is given by $N_C = (2M_1 + 1)(2M_2 + 1) \sum_{N_\uparrow=0}^N N_{SP}! / [N_\uparrow!(N_{SP} - N_\uparrow)!] N_{SP}! / [N_\downarrow!(N_{SP} - N_\downarrow)!]$. $N = N_\uparrow + N_\downarrow$ is the number of electrons (here $N = 2$), and N_{SP} is the number of single particle orbitals. To check the convergence of CI we perform exact diagonalization using single particle orbitals up to $N_{SP} = 20$. The result of this calculation and the magnetic phase diagram of Mn is summarized in Fig. 2 where the electron spin singlet-triplet phase diagram is calculated by configuration interaction method for two electrons in lateral quantum dot molecules.

Fig. 3 shows the lowest energy gap, $\Delta = E_J - E_{J=0}$, calculated for two electrons and two Mn in lateral quantum dot molecule as a function of cyclotron frequency $\omega_c = eB/m^*c$ and J . Here $\vec{J} = \vec{M} + \vec{S}$ is the total electron-Mn spin operator ($\vec{M} = \vec{M}_1 + \vec{M}_2$, and $\vec{S} = \vec{S}_1 + \vec{S}_2$ are total Mn and electron spin operators). For illustration we switched off the electron and Mn Zeeman couplings. Here the singlet-triplet transition occurs because of change in wave functions and e-e Coulomb matrix elements. Close to the transition point where the single particle energy levels of valence electrons are degenerate (half-filled), the e-e Coulomb interaction leads

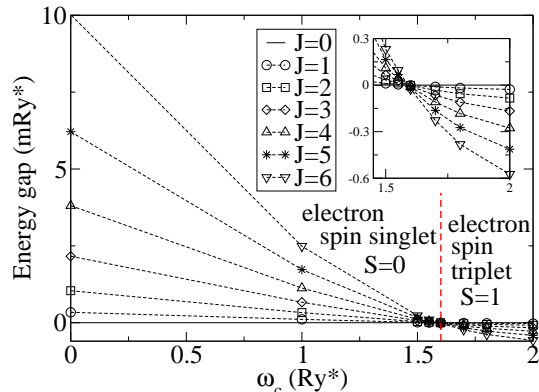


FIG. 3: (Color online) Energy gap of a system of two electrons and two Mn in lateral quantum dot molecule with $V_p = 7$ as a function of cyclotron energy (magnetic field). At $\omega_c = 1.55$ electron spin singlet-triplet transition is seen. The vertical dashed line marks the transition point. This transition induce para-ortho transition in Mn's. Below (above) this transition the ground state is identified by total angular momentum $J = 0$ ($J = 6$). A magnified part of main figure is shown in inset.

singlet-triplet transition in accordance with spin Hund's rule. The eigenvalues of H are grouped into $J = 0, \dots, 6$. States with given J are $2J + 1$ -fold degenerate. It is convenient to characterize these states based on the total spin of electrons, e.g., spin singlet ($S = 0$) and triplet ($S = 1$) and total spin of two Mn with $M = 0, \dots, 5$. In this work we are interested in the magnetic ordering of two Mn that can be described by anti-ferromagnetic, ferromagnetic and canted states corresponding to $M = 0$, $M = 5$, and $M = 1, \dots, 4$. As it is shown in Fig. 3 spin of electrons undergo singlet-triplet transition at $\omega_c^* = 1.55$ and $V_p = 7$. Within $\omega_c < \omega_c^*$, $J = M = S = 0$ is the non-degenerate ground state. At $\omega_c = \omega_c^*$, the energy gap of anti-ferromagnetic, ferromagnetic and canted states vanish all together and the ground state switches to ferromagnetic state with maximum spin multiplicity corresponding to $J = 6$, $M = 5$, and $S = 1$. In the limit of strong magnetic field there are $2J + 1 = 13$ degenerate states that form the ground state. However this degeneracy is removed by Zeeman coupling that guarantees the uniqueness of the ground state with $M_z = -5$ and $S_z = -1$. Within the resolution of our exact diagonalization we did not observe any range of magnetic field that the ground state exhibits canted ordering. In Fig. 3 at $B = 0$ and $V_p = 7$ we compare the energy gap calculated using CI, $E_{J=6} - E_{J=0} = 10$ mRy*, with perturbation approach. We find $\Delta_{ST}^{(e)} = 0.013$, $\Delta_{12} = 0.38$, hence $E_{J=6} - E_{J=0} = 11.4$ all in mRy*, in qualitative agreement with exact energy gap.

V. CONCLUSION

In this work we studied phase diagram of quantum dot molecules consist of two electrons and two magnetic impurities (Mn) confined in each dot. We demonstrated that the spin singlet-triplet transition of two electrons that are controlled by external electric gate voltage and magnetic field, can induce ferromagnetic-antiferromagnetic transition in the magnetic impurity system. Therefore, Mn-Mn spin transitions mediated by e-Mn exchange interaction can be controlled indirectly by external electric gate voltage and magnetic field. This allows us to suggest application of spin of magnetic impurities for the entanglement of qubits in quantum information processing. The advantage of using spin of magnetic impurities as qubit, instead of QD electrons resides in the possibility in achieving higher spin coherence time. In analogous to the magnetic moment of nuclear impurities in host semiconductor systems, we speculated that the spin coherence time in the Mn system is expected to be longer than the QD electron system due to small localization length of Mn d-orbitals that suppresses the qubit spin-orbit coupling as well as hyperfine interaction with the magnetic moment of nuclei of host semiconductor. Our analysis based on exact diagonaliza-

tion allows mapping the electron-electron and electron-Mn Hamiltonian H into an effective Mn-Mn Heisenberg Hamiltonian $H_{mm}^{\text{eff}} = \Delta_{12} \vec{M}_1 \cdot \vec{M}_2$ in agreement with the perturbative results, e.g., an RKKY model calculated for weak coupling at low magnetic fields. Consistent with the magnetic field dependence of the lowest lying states of full Hamiltonian H , Δ_{12} changes sign at critical magnetic field that leads to spin singlet-triplet transition of two electrons in lateral quantum dot molecules. This is a level crossing that results to para-ortho transition induced by electrons in artificial H_2 molecules where the magnetic impurities resembling the magnetic moment of nucleus of the actual H_2 molecules, and the interaction between two Mn at high magnetic field is determined by the magnetic polaron effect.

VI. ACKNOWLEDGMENT

Author acknowledges partial support from the US ONR Grants N00014-06-1-0616, N00014-06-1-0123, and NSF ECCS, and thanks Thomas Brabec, Sasha Govorov, Pawel Hawrylak, Miguel Angel Martin-Delgado, Andre Petukhov, Dean Sherry, and Igor Zutic for comments and discussions.

-
- ¹ L. Jacak *et al.*, *Quantum Dots* (Springer, Berlin, 1998); D. Bimberg *et al.*, *Quantum Dot Heterostructures* (John Wiley & Sons, Chichester, 1999). S. M. Reimann and M. Manninen, *Rev. Mod. Phys.* **74**, 1283 (2002), and the references therein.
- ² L. Besombes, Y. Leger, L. Maingault, D. Ferrand, H. Mariette, J. Cibert, *Phys. Rev. Lett.* **93**, 207403 (2004); *Phys. Rev. B* **71**, 161307(R) (2005); C. Le Gall *et al.*, *Phys. Rev. Lett.* **102**, 127402 (2009); Y. Leger, L. Besombes, J. Fernandez-Rossier, L. Maingault, H. Mariette, *Phys. Rev. Lett.* **97**, 107401 (2006); Y. Leger, L. Besombes, L. Maingault, D. Ferrand, H. Mariette, *Phys. Rev. Lett.* **95**, 047403 (2005).
- ³ C. Gould *et al.*, *Phys. Rev. Lett.* **97**, 017202 (2006).
- ⁴ S. Mackowski *et al.*, *Appl. Phys. Lett.* **93**, 153114 (2008).
- ⁵ D. A. Bussian, *Nature Materials* **8**, 35 (2008).
- ⁶ J. van Bree, P.M. Koenraad, J. Fernandez-Rossier, *Phys. Rev. B* **78**, 165414 (2008).
- ⁷ D. E. Reiter, T. Kuhn, V. M. Axt, *Phys. Rev. Lett.* **102**, 177403 (2009).
- ⁸ J. Fernandez-Rossier and L. Brey, *Phys. Rev. Lett.* **93**, 117201 (2004).
- ⁹ A. O. Govorov, *Phys. Rev. B* **72**, 075359 (2005); Wei Zhang, T. Dong, A.O.Govorov, *Phys. Rev. B* **76**, 075319 (2007).
- ¹⁰ F. Qu and P. Hawrylak, *Phys. Rev. Lett.* **96**, 157201 (2006).
- ¹¹ R. M. Abolfath, A. Petukhov, I. Zutic, *Phys. Rev. Lett.* **101**, 207202 (2008); R. M. Abolfath, P. Hawrylak, I. Zutic, *Phys. Rev. Lett.* **98**, 207203 (2007); *New Journal of Physics* **9**, 353 (2007).
- ¹² Shun-Jen Cheng, *Phys. Rev. B* **79**, 245301 (2009).
- ¹³ Nga T. T. Nguyen and F. M. Peeters, *Phys. Rev. B* **78**, 045321 (2008); **78**, 245311 (2008).
- ¹⁴ C. Echeverria-Arrondo, J. Perez-Conde, and A. Ayuela *Phys. Rev. B* **79**, 155319 (2009).
- ¹⁵ T. H. Oosterkamp *et al.*, *Phys. Rev. Lett.* **80**, 4951 (1998); M. Ciorga *et al.*, *Phys. Rev. Lett.* **88**, 256804 (2002); M. Piore-Ladriere *et al.*, *Phys. Rev. Lett.* **91**, 026803 (2003); J. R. Petta, A.C. Johnson, C.M. Marcus, M.P. Hanson, A.C. Gossard, *Phys. Rev. Lett.* **93**, 186802 (2004); M. Piore-Ladriere *et al.*, *Phys. Rev. B* **72**, 125307 (2005).
- ¹⁶ G. Burkard, D. Loss, D.P. DiVincenzo, *Phys. Rev. B* **59**, 2070 (1999); X. Hu and S. Das Sarma, *Phys. Rev. A* **64**, 042312 (2001); R. M. Abolfath, W. Dybalski, P. Hawrylak, *Phys. Rev. B* **73**, 075314 (2006).
- ¹⁷ L. Cywinski, W.M. Witzel, S. DasSarma, *Phys. Rev. Lett.* **102**, 057601 (2009); W. A. Coish and D. Loss, *Phys. Rev. B* **72**, 125337 (2005).
- ¹⁸ D. G. Cory *et al.*, *Phys. Rev. Lett.* **81**, 2152 (1998); M. A. Nielsen *et al.*, *Nature* **396**, 55 (1998).
- ¹⁹ B. E. Kane, *Nature* **393**, 133 (1998); A. Galindo and M. A. Martin-Delgado, *Rev. Mod. Phys.* **74**, 347 (2002).
- ²⁰ H. O. Churchill *et al.*, *Phys. Rev. Lett.* **102**, 166802 (2009); J. Fischer, B. Trauzettel, D. Loss, *Phys. Rev. B* **80**, 155401 (2009).
- ²¹ M. Carravetta, O.G. Johannessen, M.H. Levitt, *Phys. Rev. Lett.* **92**, 153003 (2004); W. S. Warren *et al.*, *Science* **323**, 1711 (2009).
- ²² J. Almeida, M. A. Martin-Delgado, and G. Sierra, *Phys. Rev. B* **79**, 115141 (2009); and references therein.
- ²³ M.A. Ruderman and C. Kittel, *Phys. Rev.* **96**, 99 (1954); T. Kasuya, *Prog. Theor. Phys.* **16**, 45 (1956); K. Yosida, *Phys. Rev.* **106**, 893 (1957).

- ²⁴ L. D. Landau, and E. M. Lifshitz, *Quantum Mechanics: Non-Relativistic Theory* (Pergamon, Oxford, 2003).
- ²⁵ Because the nuclear wave function of H₂ molecule is odd under exchange of two protons, in the gas phase, the para and ortho energy gap can be expressed as the energy difference between nuclear rotational energy levels associated with the molecular angular momentum. In the solid phase, the rotational degree of freedom of H₂ molecules is frozen, and the para and ortho states of hydrogen are degenerate. The spin degeneracy is removed by the electron-proton hyperfine interaction that is analogous to the e-Mn contact interaction in artificial H₂ quantum dot molecule.
- ²⁶ R. M. Abolfath, and Pawel Hawrylak, *J. Chem. Phys.* **125**, 034707 (2006).
- ²⁷ W. A. Coish, and J. Baugh, *Phys. Status Solidi B*, **246**, 2203 (2009).
- ²⁸ G. Dresselhaus, *Phys. Rev.* **100**, 580 (1955); E. I. Rashba, *Fiz. Tverd. Tela (Leningrad)* **2**, 1224 (1960); [*Sov. Phys. Solid State* **2**, 1109 (1960)]; Y. A. Bychkov and E. I. Rashba, *J. Phys. C* **17**, 6039 (1984).